

BUCKLING UNDER NONCONSERVATIVE LOAD: CONSERVATIVE SPATIAL CHAOS

Attila KOCSIS¹ and György KÁROLYI^{1,2}

¹Department of Structural Mechanics

²Center for Applied Mathematics and Computational Physics
Budapest University of Technology and Economics
H–1521 Budapest, Hungary

Received: Nov. 16, 2005

Abstract

Buckling of an elastic linkage under nonconservative load is investigated. There is a related initial value problem, which is conservative and chaotic, and gives valuable aid in finding the buckled shapes of the linkage. To illustrate the equilibrium configurations, the bifurcation diagram is constructed, which turns out to be a distorted version of the bifurcation diagram of the linkage under a conservative load.

Keywords: buckling, elastic linkage, nonconservative load.

1. Introduction

Since the first invention of *chaos theory*, it has been found to play a very important role in many different fields, ranging from physics through biology to engineering, among others. Since then, the word *chaos* indicates all sorts of systems that exhibit a complicated behaviour in the course of time. This behaviour can be characterized by a strong dependence on the initial conditions, what results in an unpredictable dynamics of the system in question. However, the unpredictable behaviour is caused by *deterministic* rules, which makes chaos distinct from probabilistic processes. Also, for a system to be identified as chaotic, it is required that it has only a small number of degrees of freedom [1]. Hence chaos theory deals with *dynamical systems*, that is, systems whose time evolution is governed by a small set of deterministic equations [2]. These governing equations form either continuous or discrete initial value problems, described by differential equations or so-called maps, respectively.

Here we deal with a related phenomena, addressed lately as *spatial chaos* in the literature [3]-[11]. Spatial chaos is a special form of spatial complexity, when the governing equations are reminiscent of a chaotic dynamical system, but the role of time is taken over by a spatial coordinate (e.g. arc-length).

Many examples of spatial chaos have been addressed recently. In general mathematical studies [12] or in fluid dynamical investigations [13], spatial complexity emerged as the steady state solution of time-dependent systems. In the case of buckling of elastic rods [3]-[5, 7, 14] or linkages [6],[8] [16] the role of time is

taken over by an arc-length parameter, and the shape of the buckled state may be similar to a chaotic trajectory in a certain phase space.

Another large class of problems where spatial chaos plays a role is related to biology. In this case, biological filaments—like DNA, (bio)polymers, or tendrils—may exhibit complicated spatial patterns. It is common in these examples that they have been modelled by either a continuous rod or a discrete linkage. For a large number of base-pairs it has been found that the shape of DNA molecules can be described by the Kirchhoff rod-model [17]-[21]. Also, to give account of the conformation of biopolymers, similar continuous models have been applied [22]-[25]. These continuous models are often referred to as *wormlike chains* [22, 24, 25]. In other cases discrete linkages are used to incorporate the discrete property of the molecules [26]-[32]. These models consider the base-pairs of DNA or certain parts of the biopolymer as (usually rigid) links, attached to each other by flexible connections [26, 30]-[32]. This set of models is often called *base-pair steps* or *stack of plates*.

Tendrils of plants have also been modeled by the Kirchhoff rod equations [33, 34]. This kind of modelling could give account of the ‘tendrill perversion’ (change of handedness) of helical tendrill shapes of climbing plants. Beside these examples, similar rod-like models have been suggested for filamentary bacteria [34, 35], for the buckling of polypropylene fibers during manufacturing non-woven fabrics [36], and for nanofibers grown on various surfaces of confined geometry [37].

The difficulty of—and the interest in—these problems lies in that to find the equilibrium shape of the rod one may have to cope with substantial computational difficulties, depending on the boundary conditions and the details of the problem. This is the consequence of the system being spatially chaotic. It seems thus advantageous to look for problems where the solutions are more easily gained, meanwhile gathering insight into the nature of spatial chaos. One such problem concerns the buckling of elastic linkages, extensively studied in the last few years [6]-[16].

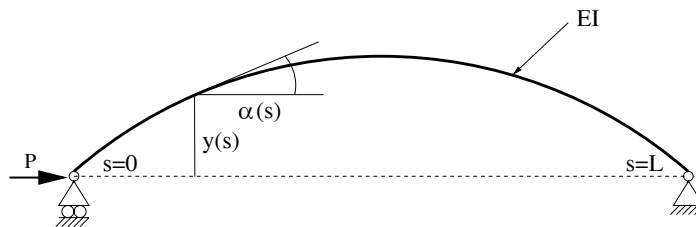


Fig. 1. Euler's buckling problem. A continuous, elastic rod of length L and bending stiffness EI is compressed by the horizontal load P . For large enough load, the initial, straight configuration becomes unstable, and other, curved equilibrium shapes emerge. These are characterized by the distance $y(s)$ from the initial configuration and the angle $\alpha(s)$ of the tangent with the horizontal, both are functions of arc-length s .

An interesting feature of elastic linkages is that they provide both a mathematical discretization of Euler's buckling problem and a mechanical discretization of a continuous rod [6, 9, 10, 16]. The set of equilibrium configurations is best visualized on *bifurcation diagrams*, where the initial angle of the rod or the linkage in equilibrium is plotted as a function of the load acting on the structure. For example, for the rod shown in *Fig. 1* a part of the bifurcation diagram is shown in *Fig. 2*. Similarly, for a linkage (illustrated in *Fig. 3*), of $N = 4$ elements *Fig. 4* shows a bifurcation diagram. Evidently the discrete problem, the elastic linkage, has much more possible equilibrium shapes than has the continuous Euler-problem. The dramatic difference between the two bifurcation diagrams is caused by the fact that the governing equations of the continuous problem coincide with a non-chaotic initial value problem, the mathematical pendulum, while the equations of the linkage are essentially the same as the well-known chaotic map, the *standard map*. This results in the appearance of so-called parasitic solutions on the bifurcation diagram of the discrete problem: these are solutions of the discrete problem, but do not correspond to any of the solutions of the continuous problem. Such 'spurious' solutions, appearing as a result of discretization, have already been found in different problems [38, 39, 40].

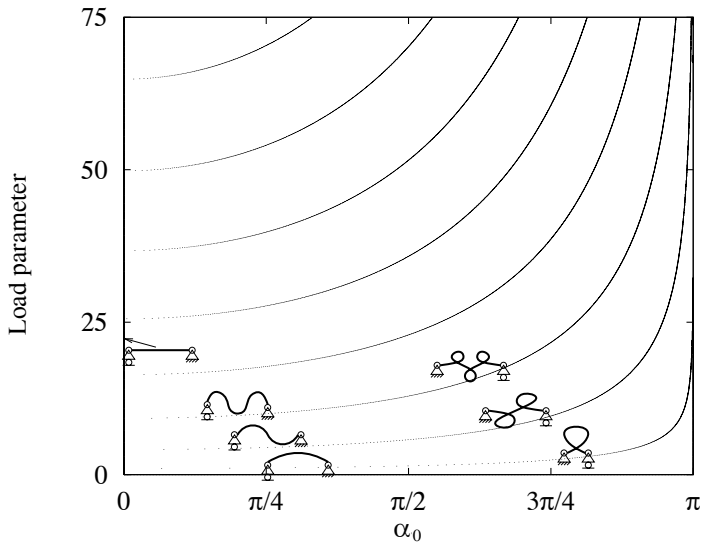


Fig. 2. Bifurcation diagram of the buckled, continuous rod. For each load value, the initial angles α_0 of the equilibrium shapes are plotted. Some buckled configurations are also shown.

Investigating the behaviour of the elastic linkages, an important result was a *symbolic dynamics* based integer labeling of the equilibrium branches of the bifurcation diagram [9, 16]. This labeling gives a complete and unique description

of all the branches [9]. Moreover, all the classical characteristics of the solutions (like symmetry properties, stability, and number of nodes) can be determined easily from the labels [10].

The buckling of linkages, as investigated before, is a conservative problem. The corresponding initial value problem, the standard map, is also conservative, in other words, it is area-preserving [6]. In this paper, we modify the original problem slightly, and we end up with a *nonconservative* buckling problem. We show that it results in a *conservative* initial value problem. Despite the difference between the original linkage problem and our nonconservative one, the equilibrium branches of the two bifurcation diagrams have a one-to-one correspondence, they are just the distorted versions of each other. This proves that spatial chaos is not a unique feature of conservative problems.

2. Buckling of Linkages

First, we briefly recall the discrete buckling problem introduced in Refs. [6, 9, 10, 11, 16]. The model consists of N rigid links of equal length ℓ . They are interconnected by hinges, which are equipped by rotational springs of stiffness ϱ . One end (at the N th hinge) is simply supported, the other end can move along the horizontal line connecting the two supports as shown in Fig. 3. The end with the roller is loaded by a force P , which always acts horizontally. In the unloaded case ($P = 0$) the configuration is straight, in that position the rotational springs are unstretched [6, 9]. With the increase of the load, buckling occurs: the original, straight configuration becomes unstable, and other equilibrium configurations appear, their number increasing rapidly with P , as illustrated in Fig. 4.

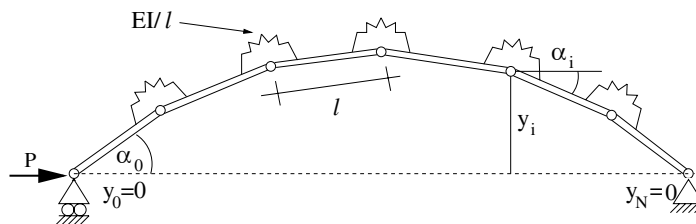


Fig. 3. Originally straight elastic linkage under compressive force P . The rigid links of length ℓ are connected to each other by hinges equipped with rotational springs of spring constant ϱ . If the spring constant ϱ is chosen to be EI/ℓ , the linkage is a discrete model of Euler's problem. The buckled configuration is characterized by the angles α_i of the links with the horizontal, and by the distances y_i of the hinges from the original straight, horizontal configuration.

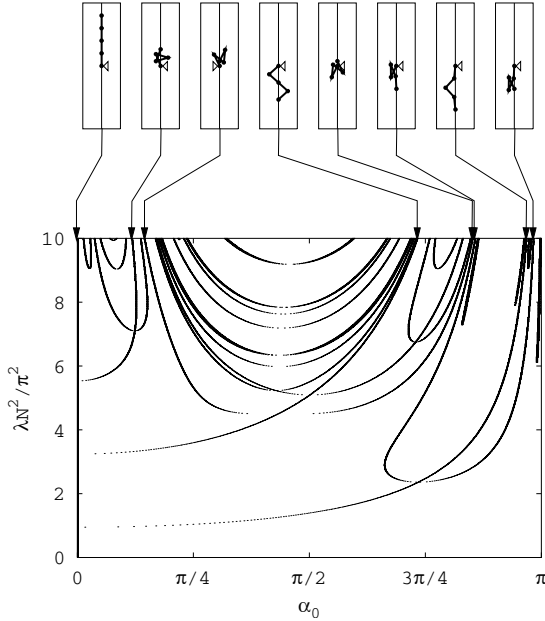


Fig. 4. Bifurcation diagram of an elastic linkage of $N = 4$ elements. For all values of the load parameter λ , the initial angles α_0 of all equilibrium configurations are plotted. Some buckled configurations are also illustrated.

Writing the equilibrium and the geometric equations of this structure in dimensionless form [9, 10], we find

$$\alpha_{i+1} = \alpha_i - \lambda y_{i+1}, \quad y_{i+1} = y_i + \sin \alpha_i \quad (1)$$

as the governing equations of the system. Here α_i is the angle of the i th link with the horizontal connecting the supports, y_i is the distance of the i th hinge from the same horizontal divided by ℓ (i.e., ℓy_i is the distance). The load parameter λ is defined as $\lambda = P\ell/\varrho$, that is, as the dimensionless ratio of the load to the spring constant. The first of Eqs. (1) is the balance of moments acting on a part of the chain, the second comes from simple geometry. These equations, together with the boundary conditions

$$y_0 = y_N = 0, \quad (2)$$

form a discrete boundary value problem. This problem is *conservative*, the internal work of the springs and the external work of the constant load are path independent.

Equations (1) can also be considered as an initial value problem, a so-called *map*: choosing initial values y_0 and α_0 , one can unambiguously compute the subsequent y_i and α_i values from (1). This mapping turned out to be connected to the

well-known *standard map* [41] by a linear transformation [6, 9, 10]. The standard map is a conservative, chaotic dynamical system [41], this causes the appearance of the large number of solutions on the bifurcation diagram of the linkage, see *Fig. 4*.

Now we modify the original problem, namely, a different load will act on the structure. Instead of being always horizontal, we choose load P to be always parallel with the first link. That is, it becomes a *follower load*. In a simplistic way, this modified system models a discrete pipe conveying fluid, the follower load mimicking the repercussion due to outflow [42]. Note that more precise models [43, 44, 45, 46] of pipes conveying fluid lead to moments at the connections different from our moments in the springs, nevertheless Ref. [42] uses a model very similar to our one.

If load P is always parallel to the first link, its vertical component is taken up by the support. Hence the problem is reduced to the original one by saying that there is a load $P \cos \alpha_0$ acting on the structure. At first this seems to be a minor modification, but it has important consequences on the problem. For example, the conservative nature of the problem is lost: the work done by the external load is path-dependent. Imagine that while the follower load P acts parallel with the first element, the first two elements are folded to a certain angle, see step 1 in *Fig. 5*. Meanwhile load P performed some work, but less than it would have worked if it had been always horizontal. Then we move the first three elements of the linkage such that the first one rotates around the support to become horizontal, while the next two becomes inclined, see step 2 in *Fig. 5*. During these steps the load does not perform work, since the starting point of the structure does not move. Then, keeping the first element horizontal, we stretch the linkage to its original, straight configuration as shown in step 3 in *Fig. 5*. During this step the load performs more negative work than it performed while folding the linkage, so the total work done is nonzero while returning to the original position.

The equations of this modified, nonconservative system are almost the same as those of the original, *Eq. (1)*. The only modification comes from that the load is now $P \cos \alpha_0$. Hence the governing equations are

$$\alpha_{i+1} = \alpha_i - \lambda y_{i+1} \cos \alpha_0, \quad y_{i+1} = y_i + \sin \alpha_i. \quad (3)$$

The boundary conditions are the same as those for the original problem, see *Eq. (2)*.

The solutions can be uniquely characterized by the initial angle α_0 for any given load. The position of the first link is given by $y_0 = 0$ and α_0 , that of the others can be computed from (3). Hence we can plot all the solutions on a bifurcation diagram that assigns the initial angle of all solutions to the corresponding λ , just like in the case of the original, conservative linkage problem. When constructing the bifurcation diagram of this modified problem, we take advantage of some symmetries. It is easy to see that if some α_0 is a solution for a certain λ , then $\alpha_0 + 2\pi$ gives the same solution (a rigid body rotation in physical space), which results in a 2π -shift symmetric (α_0, λ) bifurcation diagram. Also, if α_0 is a solution, $-\alpha_0$ or $\pi - \alpha_0$, respectively, give mirror images of the solution with respect to the horizontal or to the vertical axis, respectively. These symmetries together result in that

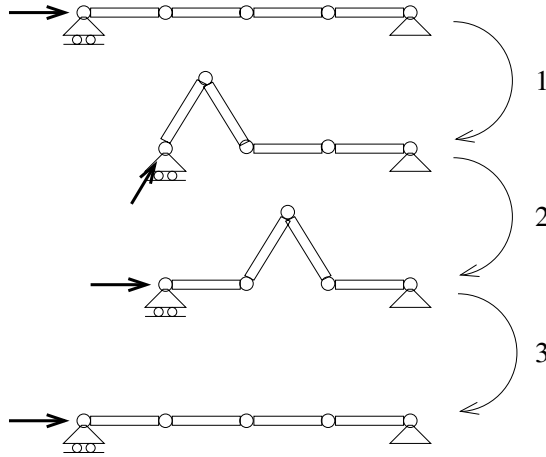


Fig. 5. The external work done in step 2 is zero, and the work is not equal in steps 1 and 3. Hence the total work is not zero, but the linkage returns into its original position. That is, the system is not conservative. Note that the configurations shown are not necessarily equilibrium configurations.

the bifurcation diagram is π -shift symmetric in α_0 , and that in the $[0, \pi]$ range it is symmetric to the $\alpha_0 = \pi/2$ line. Hence it is enough to consider α_0 between 0 and $\pi/2$. For simplicity, we restrict our attention to $\lambda > 0$, that is, to forces compressive on the first link.

When viewed as an initial value problem, *Eq. (3)* gives an area-preserving, conservative map, which is chaotic, see *Fig. 6* for the phase portrait of this map. It is clearly visible that there are large KAM islands surrounded by chaotic islands, a unique feature of conservative chaos [1, 2, 41]. For a fixed initial angle α_0 , we can take map (3) to be the same as (1), which is known to be conservative: the Jacobian of map (1) has unit determinant. It means that the modified map (3) also possesses a Jacobian with unit determinant for all fixed initial angles, hence it is area-preserving, that is, conservative.

Thus we have a nonconservative static buckling problem, which is related to a conservative, chaotic initial value problem. In the next sections, we solve the buckling problem, and construct its bifurcation diagram for some number of links N .

3. Linkage consisting of two elements

The $N = 2$ case can be treated analytically. In this case (3) leads to

$$y_1 = \sin \alpha_0, \quad \alpha_1 = \alpha_0 - \lambda \cos \alpha_0 \sin \alpha_0, \quad (4)$$

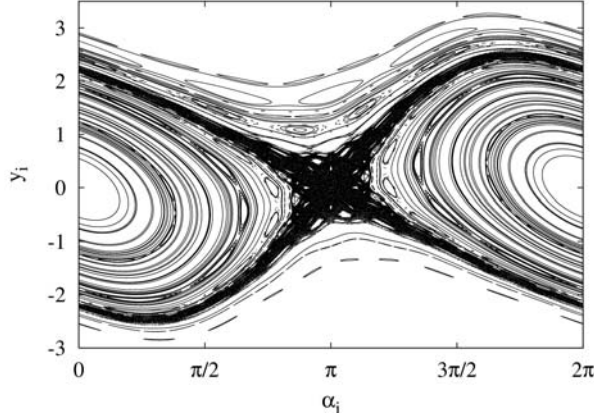


Fig. 6. Phase portrait of Eqs. (3) as an initial value problem. The value of the load parameter was $\lambda = 10$, and 100 random initial conditions were iterated 20000 times, and all the iterations plotted. The existence of invariant, closed curves (KAM islands) surrounded by chaotic sea makes it plausible that the system is in the state of conservative chaos.

while boundary condition $y_2 = 0$ becomes

$$y_2 = \sin \alpha_0 + \sin \alpha_1 = 0. \quad (5)$$

This admits two types of solutions.

The first type of solutions is $\alpha_1 = -\alpha_0 + 2k\pi$, into which *Eq. (4)* can be substituted and the following analytical expression is obtained:

$$2\alpha_0 = \frac{\lambda}{2} \sin(2\alpha_0) + 2k\pi. \quad (6)$$

The equation of the equilibrium paths in the (α_0, λ) plane become

$$\lambda(\alpha_0) = \frac{4\alpha_0 - 4k\pi}{\sin(2\alpha_0)}. \quad (7)$$

These curves are illustrated in *Fig. 7* by solid lines.

For $k > 0$ no solution exists if $\lambda > 0$ and $\alpha_0 \in [0, \pi/2]$. If $k = 0$ and $\lambda < 2$ only the trivial solution $\alpha_0 = \alpha_1 = 0$ exists. At $\lambda = 2$ a bifurcation occurs, and a nontrivial branch of solutions emerges. For any $k < 0$, if λ is smaller than a critical value depending on k , no solution exists. If λ is increased above the critical value, two new solutions appear for each $k < 0$. The new branches appear where

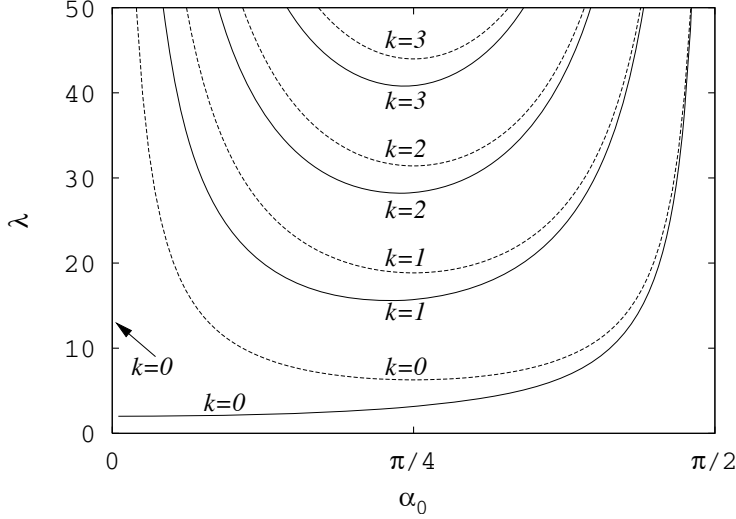


Fig. 7. Bifurcation diagram for the nonconservative linkage problem. The linkage was of $N = 2$ elements. The dashed and solid lines indicate the two different types of solutions explained in the text.

the tangent of curve (7) is horizontal. Equating to zero the derivative of (7) with respect to α_0 we find that the bifurcation appears at the α_0 satisfying

$$\tan(2\alpha_0) = 2\alpha_0 - 2k\pi, \quad (8)$$

which occurs at the critical load parameter

$$\lambda = \frac{2}{\cos(2\alpha_0)}. \quad (9)$$

The α_0 value of the bifurcation point converges to $\pi/4$ as k is increased.

The second type of solutions writes as $\alpha_1 = \alpha_0 - \pi - 2k\pi$. Using (4) results in

$$\frac{\lambda}{2} \sin(2\alpha_0) = \pi + 2k\pi. \quad (10)$$

The equation of the equilibrium branches in the (α_0, λ) plane are

$$\lambda(\alpha_0) = \frac{2\pi + 4k\pi}{\sin(2\alpha_0)} \quad (11)$$

These curves are illustrated in *Fig. 7* with dashed lines.

For $k < 0$ no solution exists if $\lambda > 0$ and $\alpha_0 \in [0, \pi/2]$. For a fixed $k \geq 0$, if λ is smaller than a critical value, no solution exists. The solutions appear when the branches have a horizontal tangent, that is, where the derivative of (11) is zero. From this condition we find that the branches appear at

$$\alpha_0 = \pi/4, \quad \lambda = 2\pi + 4k\pi. \quad (12)$$

4. Long linkages ($N > 2$)

Because map (3) is chaotic, it is not possible to find the equilibrium states analytically for arbitrary N . There is, however, a quite simple numerical method [6, 47] that is able to find the solutions with arbitrary precision. Fixing N and λ (the two dimensionless parameters of the problem) we take $y_0 = 0$ and change α_0 in small increments between 0 and $\pi/2$, that is, in the range where we want to find the solutions. Using map (3) we then find y_N . If $y_N = 0$, then the current α_0 provides a solution for the boundary value problem. If the sign of y_N is different from that resulted from the previous α_0 , there must be a solution between the previous and the current α_0 , and a suitable interpolation gives an approximate solution. If the increment in α_0 is small enough, we can find *all* solutions. Completeness may be checked by a further refinement of the increments.

Repeating this numerical scheme for several fixed load values λ provides us with the bifurcation diagram. For a linkage of $N = 4$ elements the bifurcation diagram is shown in *Fig. 8*.

The nonconservative linkage is in the state of spatial chaos, which is evident from the large number of equilibrium branches on the bifurcation diagram, even for this quite small number of links. The bifurcation diagram is similar to that shown in *Fig. 4* for the conservative case.

In fact, the similarity can be exploited further. Choose a fixed α_0 , and take the parameter of the conservative case to be $\tilde{\lambda} = \lambda \cos \alpha_0$. Then the trajectory of the original map (1) with parameter $\tilde{\lambda}$ and with initial conditions $y_0 = 0$ and α_0 become exactly the same as the trajectory of the modified map (3) with the same initial conditions, but with parameter λ . This means that if α_0 is a solution of the original buckling problem with parameter $\tilde{\lambda}$, then it also solves the modified buckling problem with parameter $\lambda = \tilde{\lambda} / \cos \alpha_0$. This observation can be readily verified in *Fig. 9*, where a distorted bifurcation diagram for the original, conservative linkage is shown. The distortion lies in the fact that on the vertical axis the values of $\lambda / \cos \alpha_0$ are measured instead of λ . In other words, the branches of *Fig. 4* are ‘grabbed’ at $\alpha_0 = \pi/2$ and ‘pulled to infinity’. This distorted bifurcation diagram of the original, conservative linkage is exactly the same as the bifurcation diagram of the nonconservative, modified problem, compare *Figs. 8* and *9*.

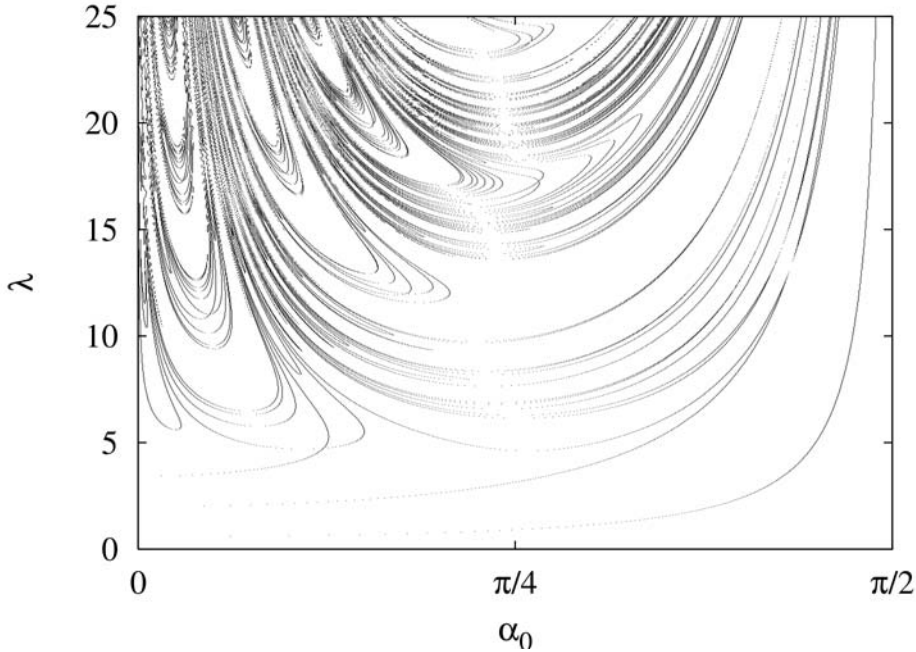


Fig. 8. Bifurcation diagram of the nonconservative linkage of $N = 4$ links.

5. Conclusions and Future Work

The main goal of this paper was to show that spatial chaos is not restricted to conservative systems. To this end, we have modified the linkage problem previously studied in detail, changing the load to be always parallel with the first link. This change had the consequence that the problem became nonconservative.

We claim that the complex bifurcation diagram, a clear sign of spatial chaos, is the consequence of an underlying chaotic initial value problem, whose governing equations are the same as those of the static buckling problem. We have shown that it is so both in case of a conservative and of a nonconservative system. We also pointed out that the underlying initial value problem of both systems is conservative. It means that we introduced a nonconservative static buckling problem which is related closely to a conservative dynamical system.

It has been shown that the bifurcation diagrams of the original and the modified problems are just the distorted versions of each other. There is a one-to-one correspondence between the equilibrium branches of the two diagrams: the bifurcation diagrams are topologically equivalent. An interesting question remains, however, which can be the subject of future investigations, regarding the symbolic dynamics based labeling already used for the original problem. It is not clear whether the

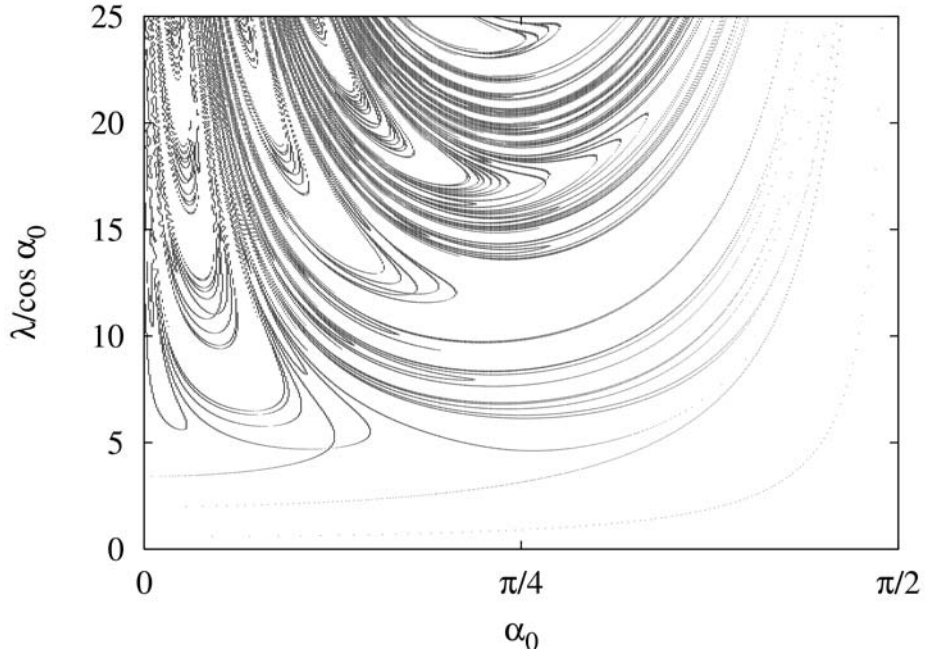


Fig. 9. The distorted version of the bifurcation diagram of the original, conservative buckling problem. The vertical axis is divided by the cosine of the initial angle α_0 . This way we end up exactly with the bifurcation diagram of the modified linkage problem, compare with *Fig. 8*.

labeling changes by the change of the loading. It is also not trivial how the labels are related to the classical invariants (like stability, symmetries, number of nodes) traditionally used to characterize equilibrium branches.

In this paper we studied a nonconservative static problem that was related to a conservative, area-preserving map. We conjecture that there is *no* relation between the conservativeness of the static problem and its related dynamic problem, and it is possible to construct either conservative or nonconservative static problems with either conservative or nonconservative corresponding dynamical problems. It could also be of interest to investigate other types of systems: for example, systems where not only the static buckling problem, but the corresponding initial value problem are nonconservative. This question has also been left for future work.

Acknowledgement

We are indebted to Zs. Gáspár, G. Domokos and T. Tél for valuable discussions. We thank the financial support from OTKA grant nos. F 042476 and T 046646. Gy. K. was supported by the Bolyai research grant, which is hereby gratefully acknowledged.

References

- [1] TÉL, T.– GRUIZ, M., *Kaotikus dinamika*. Nemzeti Tankönyvkiadó, Budapest, 2002. (In Hungarian).
- [2] OTT, E., *Chaos in dynamical systems*. Cambridge University Press, Cambridge, UK, 1993.
- [3] MIELKE, A.– HOLMES, P., Spatially Complex Equilibria of Buckled Rods. *Archives of Rational Mechanics and Analysis* **101** (1988) pp. 319–348.
- [4] THOMPSON, J. M. T. – VIRGIN, L. N., Spatial Chaos and Localization Phenomena in Non-linear Elasticity. *Physics Letters A* **126** (1988) pp. 491–496.
- [5] EL NASCHIE, M.S., On the Susceptibility of Local Elastic Buckling to Chaos. *ZAMM* **70** (1990) pp. 535–542.
- [6] DOMOKOS, G. – HOLMES, P., Euler’s Problem, Euler’s Method, and the Standard Map; or, the Discrete Charm of Buckling. *Journal of Nonlinear Science* **3** (1993) pp. 109–151.
- [7] DAVIES, M. A.– MOON, F.C., 3D Spatial Chaos in the Elastica and the Spinning Top: Kirchhoff Analogy. *Chaos* **3** (1993) pp. 93–99.
- [8] HUNT, G.W. – LAWTHORPE, R.– PROVIDÊNCIA, P. – COSTA, E., Finite Element Modelling of Spatially Chaotic Structures. *International Journal for Numerical Methods in Engineering* **40** (1997) pp. 2237–2256.
- [9] Gy. Károlyi, G. Domokos: Symbolic dynamics of infinite depth: finding global invariants for BVPs. *Physica D* **134** (1999) 316–336.
- [10] KAPSZA, E.– KÁROLYI, GY.– KOVÁCS, S.– DOMOKOS, G., Regular and Random Patterns in Complex Bifurcation Diagrams. *Discrete and Continuous Dynamical Systems B* **3** (2003) pp. 519–540.
- [11] KÁROLYI, GY., Létezik-e térbeli káosz? Locsolócső és DNS. *Természet Világa* **134** (2003) pp. 440–443. (In Hungarian)
- [12] ALBEVERIO, S.– NIZHNIK, I. L., Spatial Chaos in a Fourth-order Nonlinear Parabolic Equation. *Physics Letters A* **288** (2001) pp. 299–304.
- [13] EGUÍLUZ, V.M. – HERNÁNDEZ-GARCÍA, E.– PIRO, O. – BALLE, S., Frozen Spatial Chaos Induced by Boundaries. *Physical Review E* **60** (1999) pp. 6571–6579.
- [14] DOMOKOS, G. – HOLMES, P., On Non-inflectional Solutions of Non-uniform Elasticae. *International Journal of Non-Linear Mechanics* **28** (1993) pp. 677–685.
- [15] GÁSPÁR, ZS. – DOMOKOS, G., Global Investigation of Discrete Models of the Euler Buckling Problem. *Acta Technica Acad. Sci. Hung.* **102** (1989) pp. 227–238.
- [16] DOMOKOS, G., Static Solitary Waves as Limits of Discretization: a Plausible Argument. *Philosophical Transactions of the Royal Society of London A* **355** (1997) pp. 2099–2116.
- [17] COLEMAN, B. D.– TOBIAS, I.– SWIGON, D., Theory of the Influence of End Conditions on Self-contact in DNA Loops. *Journal of Chemical Physics* **103** (1995) pp. 9101–9109.
- [18] LIPNIACKI, T., Non-linear Mechanical Model of DNA Dynamics. *Il Nuovo Cimento D* **20** (1998) pp. 833–843.
- [19] LIPNIACKI, T., Chemically Driven Traveling Waves in DNA. *Physical Review E* **60** (1999) pp. 7253–7261.
- [20] TOBIAS, I. – SWIGON, D.– COLEMAN, B. D., Elastic Stability of DNA Configurations. I. General theory. *Physical Review E* **61** (2000) pp. 747–758.
- [21] COLEMAN, B. D.– SWIGON, D.– TOBIAS, I., Elastic Stability of DNA Configurations. II. Supercoiled Plasmids with Self-contact. *Physical Review E* **61** (2000) pp. 759–770.

- [22] KROY, K. – FREY, E., Force-extension Relation and Plateau Modulus for Wormlike Chains. *Physical Review Letters* **77** (1996) pp. 306–309.
- [23] ZÓRSKI, H. – INFELD, E. Continuum dynamics of a peptide chain. *International Journal of Non-linear Mechanics* **32** (1997) pp. 769–801.
- [24] SAMUAL, J. – SINHA, S., Elasticity of Semiflexible Polymers. *Physical Review E* **66** (2002) pp. 050801(R).
- [25] DHAR, A. – CHAUDHURI, D. Triple Minima in the Free Energy of Semiflexible Polymers. *Physical Review Letters* **89** (2002) pp. 065502.
- [26] MERGELL, B. – EJTEHADI, M. R. – EVERAERS, R., Modeling DNA Structure, Elasticity, and the Deformations at the Base-pair Level. *Physical Review E* **68** (2003) pp. 021911.
- [27] STORM, C. – NELSON, P.C., Theory of High-force DNA Stretching and Overstretching. *Physical Review E* **67** (2003) pp. 051906.
- [28] ÁDLAND, H. M. – MIKKELSEN, A., Brownian Dynamics Simulations of Needle Chain and Nugget Chain Polymer Models—Rigid Constraint Conditions Versus Infinitely Stiff Springs. *Journal of Chemical Physics* **120** (2004) pp. 9848–9858.
- [29] GÁSPÁR, ZS. – NÉMETH, R., Discrete Model of Twisted Rings. *Computer Assisted Mechanics and Engineering Sciences* **11** (2004) pp. 211–222.
- [30] COLEMAN, O.B.D. – OLSON, W.K. – SWIGON, D., Theory of Sequence-dependent DNA Elasticity. *Journal of Chemical Physics* **118** (2003) pp. 7127–7140.
- [31] OLSON, W. K. – SWIGON, D. – COLEMAN, B. D., Implications of the Dependence of the Elastic Properties of DNA on Nucleotide Sequence. *Philosophical Transactions of the Royal Society of London A* **362** (2004) pp. 1403–1422.
- [32] MICHELETTI, C. – BANAVAR, J.R. – MARITAN, A., Conformation of Proteins in Equilibrium. *Physical Review Letters* **87** (2001) pp. 088102.
- [33] GORIELY, A. – TABOR, M., Spontaneous Helix Hand Reversal and Tendril Perversion in Climbing Plants. *Physical Review Letters* **80** (1998) pp. 1564–1567.
- [34] GORIELY, A. – TABOR, M., The nonlinear Dynamics of Filaments. *Nonlinear Dynamics* **21** (2000) pp. 101–133.
- [35] GOLDSTEIN, R. E. – GORIELY, A. – HUBER, G. – WOLGEMUTH, C. W., Bistable helices. *Physical Review Letters* **84** (2000) pp. 1631–1634.
- [36] HÖLMES, P. – DOMOKOS, G. – SCHMITT, J. – SZEBERÉNYI, I., Constrained Euler Buckling: an Interplay of Computation and Analysis. *Computer Methods in Applied Mechanics and Engineering* **170** (1999) pp. 175–207.
- [37] HÖLMES, P. – DOMOKOS, G. – HEK, G. Euler Buckling in a Potential Field. *Journal of Non-linear Science* **10** (2000) pp. 477–505.
- [38] GAINES, R., Difference Equations Associated with Boundary Value Problems for Second Order Nonlinear Ordinary Differential Equations. *SIAM Journal of Numerical Analysis* **11** (1974) pp. 411–434.
- [39] PEITGEN, H.O. – SAUPE, D. – SCHMITT, K., Nonlinear Elliptic Boundary Value Problems Versus their Finite Difference Approximations: Numerically Irrelevant Solutions. *Crelle Journal für die Reine und Angewandte* **322** (1981) pp. 174–117.
- [40] HEGEDŰS, I., Analysis of Lattice Single Layer Cylindrical Structures. *Journal of Space Structures* **2** (1986) pp. 87–89.
- [41] LICHTENBERG, A. J. – LIEBERMANN, M. A. *Regular and stochastic motion*. Springer, New York, 1982.
- [42] BOU-RABEE, N. M. – ROMERO, L.A. – SALINGER, A. G., A Multiparameter, Numerical Stability Analysis of a Standing Cantilever Conveying Fluid. *SIAM Journal of Applied Dynamical Systems* **1** (2002) pp. 190–214.
- [43] SZABÓ, ZS., *Nonlinear vibrations of parametrically excited complex mechanical systems*. PhD dissertation, Budapest University of Technology and Economics, 2001.
- [44] SZABÓ, ZS., Parametric excitation of pipes through fluid flow. *Computer Assisted Mechanics and Engineering Sciences* **6** (1999) pp. 487–494.
- [45] SZABÓ, ZS., Bifurcation Analysis of a Pipe Containing Pulsatile Flow. *Periodica Polytechnica* **44** (2000) pp. 149–160.
- [46] SZABÓ, ZS., Nonlinear Analysis of a Cantilever Pipe Containing Pulsatile Flow. *Meccanica* **38** (2003) pp. 161–172.
- [47] DOMOKOS, G. Computer Experiments with Elastic Chains. *Newsletter of the Technical University of Budapest* **9** (1991) pp. 14–26.